A&A 507, 693–704 (2009)
DOI: 10.1051/0004-6361/200912024

Astronomy & Astrophysics

The infrared emission of ultraviolet-selected galaxies from $z = 0$ to $z = 1$

V. Buat[1], T. T. Takeuchi[2], D. Burgarella[1], E. Giovannoli[1], and K. L. Murata[3]

[1] Laboratoire d'Astrophysique de Marseille, OAMP, Université Aix-Marseille, CNRS, 38 rue Frédéric Joliot-Curie, 13388 Marseille Cedex 13, France
e-mail: [veronique.buat;denis.burgarella;elodie.giovannoli]@oamp.fr
[2] Institute for Advanced Research, Nagoya University, Japan
e-mail: takeuchi@iar.nagoya-u.ac.jp
[3] Division of Particle and Astrophysical Sciences, Nagoya University, Japan
e-mail: murata.katsuhiro@g.mbox.nagoya-u.ac.jp

Received 10 March 2009 / Accepted 16 July 2009

ABSTRACT

Aims. We want to study the IR (>8 μm) emission of galaxies selected on the basis of their rest-frame UV light in a very homogeneous way (wavelength and luminosity) from $z = 0$ to $z = 1$. We compare their UV and IR rest-frame emission to study the evolution in dust attenuation with z as well as to check if a UV selection is capable of tracking all star formation. This UV selection will also be compared to a sample of Lyman break galaxies selected at $z \simeq 1$.

Methods. We select galaxies in UV (1500–1800 Å) rest-frame at $z = 0$, $z = 0.6$–0.8, $z = 0.8$–1.2, and with as Lyman break galaxies at $z = 0.9$–1.3, the samples are compiled to sample the same range of luminosity at any redshift. The UV rest-frame data come from GALEX for $z < 1$ and the U-band of the EIS survey (at $z = 1$). The UV data are combined with the IRAS 60 μm observations at $z = 0$ and the Spitzer data at 24 μm for $z > 0$ sources. The evolution in the IR and UV luminosities with z is analysed for individual galaxies as well as in terms of luminosity functions.

Results. The $L_{\rm IR}/L_{\rm UV}$ ratio is used to measure dust attenuation. This ratio does not seem to evolve significantly with z for the bulk of our sample galaxies, but some trends are found for both galaxies with a strong dust attenuation and UV luminous sources: galaxies with $L_{\rm IR}/L_{\rm UV} > 10$ are more frequent at $z > 0$ than at $z = 0$, and the largest values of $L_{\rm IR}/L_{\rm UV}$ are found for UV faint objects; in contrast, the most luminous galaxies of our samples ($L_{\rm UV} > 2 \times 10^{10}$ $L_{\odot}$), detected at $z = 1$, exhibit a lower dust attenuation than fainter ones. The value of $L_{\rm IR}/L_{\rm UV}$ increases with the K rest-frame luminosity of the galaxies at all redshifts considered and shows a residual anticorrelation with $L_{\rm UV}$. The most massive and UV luminous galaxies exhibit quite high specific star formation rates. Lyman break galaxies exhibit systematically lower dust attenuation than UV-selected galaxies of same luminosity, but similar specific star formation rates. The analysis of the UV + IR luminosity functions leads to the conclusion that up to $z = 1$, most of the star formation activity of UV-selected galaxies is emitted in IR. Although we are able to infer information about all the star formation from our UV selection at $z = 0.7$, at $z = 1$ we miss a large fraction of galaxies more luminous than $\simeq 10^{11}$ $L_{\odot}$. The effect is found to be larger for Lyman break galaxies.

Key words. galaxies: evolution – Galaxy: stellar content – infrared: galaxies – ultraviolet: galaxies

1. Introduction

The measurement of star formation rate (SFR) at various redshifts is one of the most general diagnostics for quantifying the evolution of galaxies, individually or the population as a whole. The optimal way to perform this analysis is to consider galaxy samples selected identically at different redshifts. As long as star-forming galaxies are to be selected, a UV selection is theoretically very efficient. Nevertheless, this situation can be complicated by the effects of dust attenuation. Since dust attenuation affects the measurement of star formation rate inferred from the observed UV emission, a correction (sometimes quite large) must be applied to the observed UV emission before translating it into SFR. However, the effects of dust obscuration may be even more dramatic if they lead to the non-detection of galaxies in UV surveys: in this case a correction for dust attenuation of the total light observed in UV would not be sufficient to infer the correct global star formation rate at a given redshift.

The UV (1500–1800 Å) to IR (8–1000 μm) luminosity ratio $L_{\rm IR}/L_{\rm UV}$ is now commonly used as a robust proxy of dust attenuation. The GALEX all-sky survey associated with the IRAS catalogues has produced large samples of nearby galaxies observed at both wavelengths and used to study the variation in $L_{\rm IR}/L_{\rm UV}$ with the total $L_{\rm IR} + L_{\rm UV}$ luminosity (i.e., the total SFR of galaxies). The ratio $L_{\rm IR}/L_{\rm UV}$ has been found to increase with $L_{\rm IR} + L_{\rm UV}$ (Martin et al. 2005; Buat et al. 2007a). The same relation holds in galaxies selected in either in UV or IR (Buat et al. 2007a). This confirms a general increase of dust attenuation with galaxy luminosity that had already been reported (e.g., Hopkins et al. 2001; Moustakas et al. 2006).

This relation between total luminosity and dust attenuation in galaxies is useful to correct for the systematic effects of dust attenuation in galaxy surveys. It is important to verify whether this relation still holds at higher z. Several studies have been devoted to this issue. In contrast findings for the nearby universe, it appears that the result depends on the way galaxies are selected. IR selected galaxies at intermediate redshift ($z = 0.5$–0.8) seem to follow the mean trends found at $z = 0$ between $L_{\rm IR} + L_{\rm UV}$ and $L_{\rm IR}/L_{\rm UV}$ (Choi et al. 2006; Xu et al. 2007; Zheng et al. 2006). Buat et al. (2007b) reported only a slight decrease in

dust attenuation (~0.5 mag) for luminous IR galaxies (LIRGs) at $z = 0.7$, compared to a similar sample of galaxies at $z = 0$. When galaxies are selected in UV/optical, the situation is quite different: a strong decrease in L_{IR}/L_{UV} has been reported for a given total $L_{IR}+L_{UV}$, compared to that found at $z = 0$ (Burgarella et al. 2006, 2007; Reddy et al. 2008).

The origin of this discrepancy is unclear. Do the properties of galaxies change with z and/or do we select very different galaxy populations when selecting either in UV or IR? It is worth noting that no specific difference was found between $z = 0.6$ and $z = 0$ when L_{IR}/L_{UV} was compared to L_{UV} (Xu et al. 2007).

In the nearby universe Buat et al. (2007a) showed that a UV or an IR selection produces similar results, except for intrinsically very luminous galaxies, which are under-represented in the UV samples. These objects are rare at $z = 0$, but because of the evolution of the luminosity functions with z we might expect a different situation at higher z.

To answer these questions, we gather several samples of UV-selected galaxies from $z = 0$ to $z = 1.2$, selected in a very homogeneous way. We also consider a sample of Lyman break galaxies (LBGs) selected at $z \simeq 1$ to compare with those purely UV-selected. We add IR fluxes (when available) for all the galaxies in these samples. With these data, we study the evolution with z of the IR emission mainly by the analysis of the L_{IR}/L_{UV} ratio and the measurement of the total star formation activity by combining measurements of IR and UV emissions. The reliability of UV-selected galaxies in tracing all the star formation is assessed by analyzing the bolometric ($L_{IR} + L_{UV}$) luminosity functions.

Throughout the paper we assume that $\Omega_m = 0.27$, $\Omega_\Lambda = 0.73$, and $H_0 = 71$ km s^{-1} Mpc^{-1}. All magnitudes are given in the AB system except for the R magnitude from the COMBO-17 survey (Sect. 2.1). The luminosities are defined as νL_ν and expressed in solar units assuming that $L_\odot = 3.83 \times 10^{33}$ erg s^{-1}.

2. The galaxy samples

2.1. The UV-selected samples

The samples must be purely UV-selected. As a consequence, we rely mostly on the GALEX survey for redshifts lower than 1.

At $z = 0$, we consider the IRAS/GALEX sample compiled by Buat et al. (2007a). This sample consists of galaxies selected in the GALEX *FUV* band (1530 Å) with $FUV < 17$ mag. It is a flux-limited sample and the luminosity function has been compiled down to $L_{FUV} = 10^8\ L_\odot$. The *FUV* wavelength is assumed to be the reference wavelength for samples at higher z, and quoted as UV throughout the paper.

At higher z, our samples are extracted from the GALEX deep observations of the CDFS. GALEX (Morrissey et al. 2005) observed this field in both the *FUV* (1530 Å) and the *NUV* (2310 Å) as part of its deep imaging survey. To add IR data we limit our study to the sub-field covered by Spitzer/MIPS observations as part of the GOODS key program (e.g., Elbaz et al. 2007).

The sample at $z \simeq 0.7$ was already used by Buat et al. (2008); at this redshift, the *NUV* band of GALEX at 2310 Å corresponds to the *FUV* rest frame of the galaxies. This sample thus consists of galaxies selected in *NUV* and with a redshift between 0.6 and 0.8. Redshifts were taken from the COMBO-17 survey of the field (Wolf et al. 2004). The data reduction and the cross-identification with the COMBO-17 sources is also described in Burgarella et al. (2006). For the brightest isolated sources of the field, we perform a comparison between the fluxes given by the GALEX pipeline, aperture photometry measurements, and fluxes obtained by PSF fitting with DAOPHOT. From this comparison, we conclude that the fluxes given by DAOPHOT and previously used might be slightly overestimated by 0.2 mag. Although it is unclear whether this shift is reliable for crowded objects we decided to apply the correction to all the UV data in the CDFS field: $NUV(\text{new}) = NUV(\text{old}) - 0.2$ mag. This systematic correction remains very small (of the order of the error) and does not correspond to any modification to our previous results. Although the completeness of the *NUV* data at a level of 80% is obtained for $NUV = 26$ mag, we truncate the sample at $NUV = 25.3$ mag, so that more than 80% of the GALEX sources are identified in COMBO-17 with $R < 24$ mag. This limit ensures a redshift accuracy better than 10% (Wolf et al. 2004). We also restrict the final sample to objects with a single counterpart in COMBO-17 within 2 arcsec (i.e., 90% of the UV sources). Three-hundred galaxies are thus selected. The limit of $NUV = 25.3$ mag corresponds to $\log L_{UV} = 9.3(L_\odot)$ at $z = 0.7$, and 44% (131/300) of these sources are detected at 24 μm. For undetected sources, we adopt an upper limit of 0.025 mJy (Buat et al. 2008).

At $z \simeq 1$, we must compile a new sample. The *NUV* band of GALEX corresponds to 1155 Å in the rest frame of the galaxies. Blueward of 1200 Å the spectral energy distribution of galaxies is poorly known and the few available observations have shown that the shape of the spectral energy distribution (SED) may vary significantly from galaxy to galaxy (Buat et al. 2002; Leitherer et al. 2002): the power-law model valid for $\lambda > 1200$ Å cannot be safely applied at shorter wavelengths. To avoid this difficulty we perform a U-selection. We again work in the CDFS/GOODS field and U-band observations were performed as part of the EIS survey (Arnouts et al. 2001). We cross-correlate the U-selected catalogue with the COMBO-17 sample with a tolerance radius of 1 arcsec. Redshifts were taken from COMBO-17+4 (Tapken, private communication) that provide reliable redshifts, especially at $z \geq 1$ in the GOODS-South field by combining COMBO-17 filters with three near-infrared bands in ISAAC *JHK* bands, and 69% of the U sources are identified uniquely to a faintness limit of $U = 26$ mag. We limit the sample at $U = 24.3$ mag, which corresponds to 80% of the sources identified in COMBO-17 with a single counterpart. The photometric redshifts from COMBO-17 are robust only for galaxies with $R < 24$ mag (in the Johnson system), and 96% of our galaxies fulfil this condition. We then select galaxies in the redshift bin 0.8–1.2, which results in a sample of 316 galaxies. At this redshift the U-band corresponds to ~1800 Å in the galaxy rest-frame ($z = 1$) when our reference wavelength is 1530 Å. Because of uncertainties in the shape of the UV SEDs we prefer to avoid any interpolation between the *NUV* and U observed fluxes, and use the uncorrected U data. We can estimate the uncertainty caused by the shift of the rest-frame wavelengths from 1800 to 1530 Å: by assuming a power law for the continuum between these two wavelength and for reasonable values of this power-law that are valid for a UV selection ($\alpha = -2$ to 1, where $F_\alpha \propto \lambda^\alpha$) the error is at most 20%. The limiting magnitude $U = 24.3$ mag corresponds to $\log L_{UV} = 9.9$ ($L_\odot$) at $z = 1$. As for the sample at $z = 0.6$–0.8, the 24 μm data from Spitzer/MIPS were cross-correlated with the U sources identified in COMBO-17, within a tolerance radius of 2 arcsec (Buat et al. 2008). At the end 207 of the 316 galaxies are detected at 24 μm. For undetected targets at 24 μm , we again adopt an upper limit of 0.025 mJy (Buat et al. 2008).

In this paper we aim to determine whether a UV selection is capable tracking all star formation. The comparison between

the IR and UV emissions allows us to study both the star formation and the dust attenuation affecting newly formed stars. In this context, quasars and active galaxies are excluded from all samples. We exclude objects classified as QSO/Seyfert1 in the COMBO-17 classification (2 objects at $z \simeq 0.7$ and 4 at $z \simeq 1$). We also cross-correlate our galaxy sample with the X-ray sources observed by CHANDRA in the field (Bauer et al. 2004), and we discard 22 sources at $z \simeq 0.7$ and 19 at $z \simeq 1$ as being X-ray emitters. As a final check, we compare mid-IR IRAC colours as suggested by Stern et al. (2005) to determine if our samples were still contaminated by AGNs. At $z = 0.7$ and 1, 1 and 4% of the samples respectively were found in the AGN area close to the boundary where the contamination by star-forming sources is significant. We choose not to exclude these remaining sources.

2.2. Lyman break galaxies at $z \simeq 1$

This paper presents a sample of galaxies in the CDFS-GOODS field selected to be LBGs with a similar UV selection as that used in previous works (Burgarella et al. 2006, 2007, 2009). The primary selection was performed in GALEX *NUV* band to a faintness limit of $NUV = 25.3$ mag. As discussed in Sect. 2.1, this limit allows us to ensure that 80% of the sources are identified with a reliable redshift in COMBO-17. We then search for GALEX *FUV* counterparts to $FUV = 26.8$ mag (80% completeness on the GALEX detections). To be selected as a LBG, an object must comply with the two criteria: 1) its redshift must be in the range $0.9 < z < 1.3$, and 2) its UV colour $FUV - NUV > 2$ mag. Some *NUV* faint objects that would be classified as LBGs if the *FUV* limiting magnitudes had reached to $FUV < 27.3$ mag, are not selected as LBGs in the present sample.

This selection provides 117 LBGs with a unique counterpart in the optical of which 58 are detected at 24 μm. For the remaining sources, an upper limit of 0.025 mJy is adopted as for the other samples. In addition, we have 33 LBGs with two counterparts in the optical of which 20 are detected at 24 μm.

As for the $z = 1$ sample, the UV luminosity is based on the observed U-band. At $z = 1$, the selection of galaxies based on their Lyman break focuses on galaxies with a high intrinsic UV continuum and a large intrinsic break, since the role of the intergalactic medium on the amplitude of the break is known to be low at this redshift (e.g., Malkan et al. 2003). The situation is different for LBGs selected at higher z, whose break is dominated by the effect of the intergalactic medium. Nevertheless, Burgarella et al. (2007) found similar spectral energy distributions for LBGs at $z \simeq 1$ and $z \simeq 3$.

2.3. Estimating the IR luminosities

We aim to compare the IR and UV emission of the galaxies from $z = 0$ to $z \simeq 1$. At $z = 0$, the IR (8–1000 μm) emission is estimated using the calibration of Dale et al. (2001), based on the 60 and 100 μm fluxes from IRAS (Buat et al. 2005). At higher z, we use the emission at 24 μm to estimate the total far infrared emission. At $z = 0.7$ and $z = 1$, respectively, the observed 24 μm corresponds to rest-frame $\simeq 15$ μm and 12 μm, respectively. The extrapolation from the mid-infrared (MIR) emission to the total IR emission is known to be quite difficult but, to $z = 1$, we still observe a wavelength range also observed in the nearby universe by either IRAS or ISO. As a consequence, several calibrations and IR SED templates were proposed in the literature based on observations of nearby galaxies by IRAS and/or ISO (e.g., Chary & Elbaz 2001; Dale & Helou 2002; Takeuchi et al. 2005a). The Spitzer observations have illustrated the large variety of IR spectral energy distributions in nearby galaxies (Dale et al. 2005; Rieke et al. 2008). These observations imply that there are large uncertainties in the extrapolation from a monochromatic flux to the total IR emission. To assess this uncertainty, we can compare several calibrations of the monochromatic luminosities at 12 and 15 μm into bolometric IR luminosities. We consider the calibrations of Chary & Elbaz (2001) and Dale & Helou (2002) based on templates produced by combining IRAS and ISO data on small samples of galaxies. Following the method of Marcillac et al. (2006), the Dale & Helou (2002) templates are calibrated in total IR luminosities and we obtain the following relations between total and monochromatic luminosities:

$$\log L_{\rm IR} = 1.25 \log L_{12} - 0.341, \quad (1)$$

$$\log L_{\rm IR} = 0.985 \log L_{15} + 1.26. \quad (2)$$

We also consider the calibrations of Takeuchi et al. (2005a) (hereafter TBI05) based on a statistical analysis of all the galaxies observed in the four bands of IRAS in the Point Source Catalog (Saunders et al. 2000). The relation obtained by TBI05 at $\lambda = 12$ μm for local galaxies (i.e., when we observe a galaxy at $\lambda_{\rm obs}$, its emitted wavelength $\lambda_{\rm em}$ corresponds to 12 μm at $z = 1$) is slightly modified to take into account a slight non-linearity for the most luminous objects,

$$\log L_{\rm IR} = 2.265 + 0.707 \log L_{12} + 0.014 (\log L_{12})^2, \quad (3)$$

whereas at $\lambda = 15$ μm, we used the original relation

$$\log L_{\rm IR} = 1.23 + 0.972 \log L_{15} \quad (4)$$

at $z = 0.7$, since the non-linearity is then not significant. We checked that the estimated $L_{\rm IR}$s do not differ by more than 5% compared to the old calibration presented in TBI05. We also add to the comparison the calibration obtained by Rieke et al. (2008) at 12 μm based on a compilation of Spitzer data with particular emphasis on Luminous and Ultra Luminous Infrared Galaxies (LIRGs and ULIRGs). The comparison between all of these calibrations is shown in Fig. 1. To highlight the differences, we normalized the relations to those of DH02. The rms dispersion is overplotted for each relation.

At 15 μm (corresponding to the sample at $z = 0.7$ in the present work), the calibrations of Chary & Elbaz (2001) (hereafter CE01) and Dale & Helou (2002, hereafter DH02) are found similar: the calibration of TBI05 leads to a slightly lower $L_{\rm IR}$ by about 0.1 dex than those obtained with the CE01 relation. This difference is much smaller than the intrinsic dispersion of the correlations and Buat et al. (2007b) found that both calibrations produced very similar results about dust attenuation for a sample of LIRGs. However, at 12 μm ($z = 1$) the discrepancy is found to be larger between the calibrations of CE01 and DH02 on the one hand (again very similar) and that of TBI05 on the other hand: it reaches 0.2 dex for galaxies with $L_{\rm IR} \simeq 10^{11}$ $L_\odot$, the TBI05 relation inferring systematically lower IR luminosities. Nevertheless, these relations, which are calibrated at $z = 0$, remain marginally consistent to within a margin of error of one rms, and we expect at least the same amount of dispersion at higher redshift. The relation proposed by Rieke et al. (2008) for $\log L_{\rm IR} > 8.5$ ($L_\odot$) appears to be much steeper than the others leading to higher IR luminosities especially for intrinsically luminous objects. Rieke et al. (2008) gathered SEDs of nearby LIRGs and ULIRGs and the Dale & Helou (2002) templates

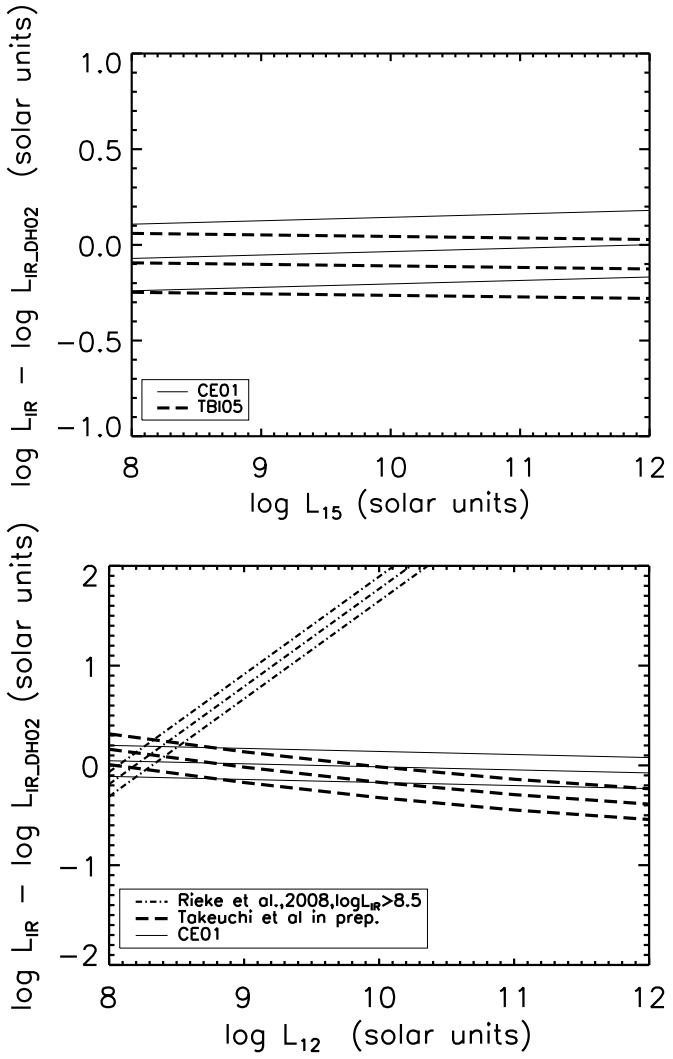

Fig. 1. Different calibrations of $\log(L_{24})$ at $z = 0.7$ (*upper panel*) – and $z = 1$ (*lower panel*) versus $\log L_{\rm IR}$. All the calibrations are normalized to the values found with the DH02 relations given in the text. The three lines plotted for each calibration correspond to the mean relation and the rms dispersion.

applied to the SINGS sample for galaxies of intermediate luminosity. Therefore, we suspect that the discrepancy between the Dale & Helou (2002) and Rieke et al. (2008) calibrations is due to the introduction of these LIRGs and ULIRGs. Once again these differences illustrate the uncertainty in these calibrations. At $z \simeq 0.7$, 26% of our galaxies detected at 24 μm and 11% of the whole sample are LIRGs-ULIRGs; at $z \simeq 1$, these fractions reach 34% of the galaxies detected at 24 μm and 22% of the whole sample. Although these fractions are significant, LIRGs-ULIRGs are not predominant in our sample and we do not use the relation of Rieke et al. (2008). We perform all analyses reported in this work for the two calibrations TBI05 and CE01. The plots are qualitatively similar and they will be presented with the TBI05 calibration. When quantitative evaluations are made (regressions or percentages), they are given for both calibrations.

3. Variation in $L_{\rm IR}/L_{\rm UV}$

As described in the introduction $L_{\rm IR}/L_{\rm UV}$ is a robust indicator of dust attenuation for galaxies that are actively forming stars. Reddy et al. (2008) and Burgarella et al. (2009) reported a clear

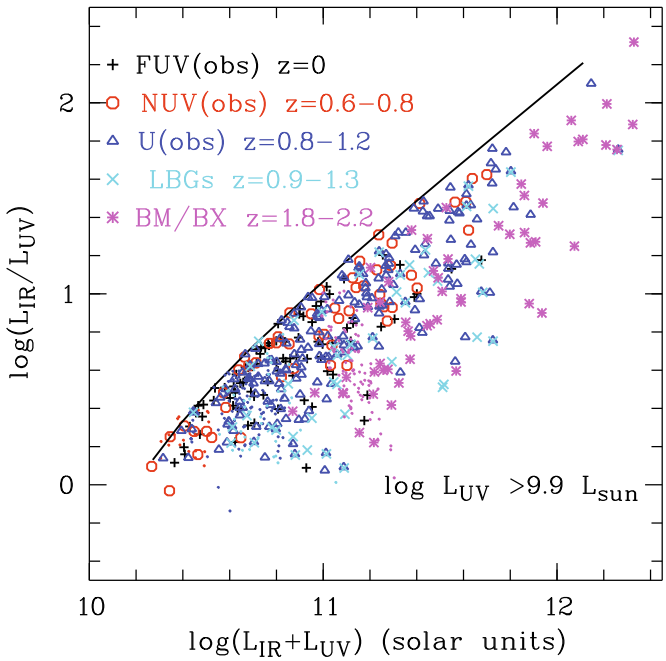

Fig. 2. $\log(L_{\rm IR}/L_{\rm UV})$ versus $\log(L_{\rm IR}+L_{\rm UV})$ for the different samples (i.e., redshifts) defined in this work and the BM/BX galaxies of Reddy et al. (2006). The different symbols corresponds to detections at 24 μm ($z = 0$: plus, $z = 0.6$–0.8: circles, $z = 0.8$–1.2: triangles, LBGs: crosses, BM/BX: stars), dots represents upper limits. The solid line corresponds to the adopted limit in UV luminosity: $\log(L_{\rm UV}[L_\odot] = 9.9)$.

decrease in this ratio for LBGs at $z = 1$ and BM/BX galaxies at $z = 2$ for a constant $L_{\rm IR} + L_{\rm UV}$ luminosity. This decrease in dust attenuation as redshift increases may have significant consequences in the search for high redshift galaxies and the measurement of their star formation rate. Here we reinvestigate this question with our homogeneous samples selected in a similar way at $z = 0$, $\simeq 0.7$, and $\simeq 1$.

3.1. $L_{\rm IR}/L_{\rm UV}$ versus $L_{\rm IR} + L_{\rm UV}$

As detailed in the previous section, the samples are all selected in UV rest-frame at wavelengths sufficiently close to avoid K-corrections. Nevertheless, the range of luminosities observed in each sample is different. Before any comparison we must apply a cut to the samples at same luminosity. The most stringent limit is that applied to the U-selected sample. With a cut at $U = 24.3$ mag, we are only able to observe galaxies with $\log L_{\rm UV} > 9.9$ ($L_\odot$) at $z = 1$. In Fig. 2 we present data for all the galaxy samples considered in this work and truncated at $\log L_{\rm UV} > 9.9$ ($L_\odot$). A trend with redshift is apparent where galaxies appear to be shifted toward the right of the plot as z increases. The mean values found for $L_{\rm IR}/L_{\rm UV}$ in the luminosity bin 10.8–11.3 ($L_\odot$) are $\langle L_{\rm IR}/L_{\rm UV}\rangle = 0.86 \pm 0.35, 1.07 \pm 0.30, 0.75 \pm 0.30$, and 0.54 ± 0.35 at $z = 0, 0.7, 1$, and for the LBG sample, respectively. Although no clear trend is confirmed between $z = 0$ and 1 given the large dispersion in the $L_{\rm IR}/L_{\rm UV}$ distribution, for a given $L_{\rm IR}+L_{\rm UV}$, dust attenuation inferred from $L_{\rm IR}/L_{\rm UV}$ is lower for LBGs at $z \simeq 1$. We also overplotted the sample of BM/BX galaxies of Reddy et al. (2006) at $z = 2$. The IR luminosities are estimated from the 24 μm fluxes using the calibration of Caputi et al. (2007), as in Reddy et al. (2008), and the UV luminosity is calculated from the G band fluxes. Given the differences between these estimates and the estimates derived in this work we do not complete a quantitative

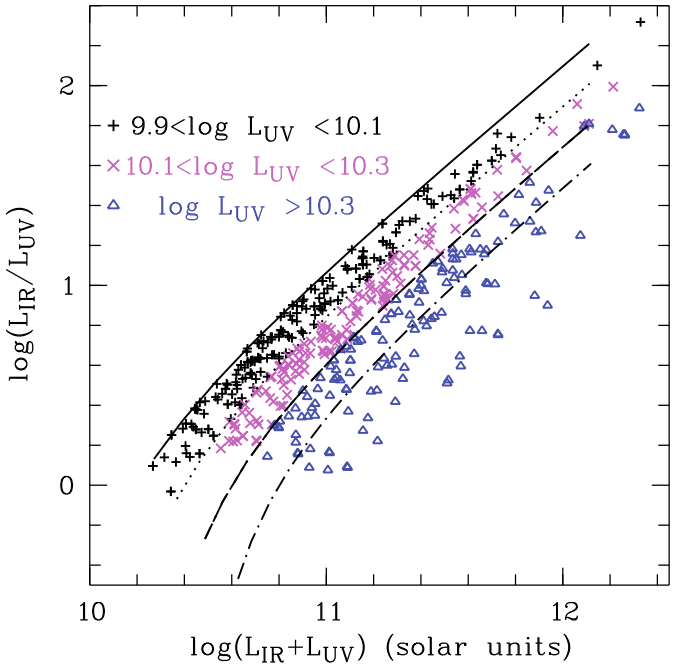

Fig. 3. $\log(L_{IR}/L_{UV})$ versus $\log(L_{IR} + L_{UV})$, 3 subsamples are defined according to the UV (rest-frame) luminosity and different symbols are used for each of them. The lines correspond to the locus of galaxies with a fixed L_{UV}: $\log L_{UV}$ = 9.9 (solid line), 10.1 (dotted line), 10.3 (dashed line), and 10.5 (dot-dashed line) in solar units. For the sake of simplicity, upper limits to 24 μm are not overplotted.

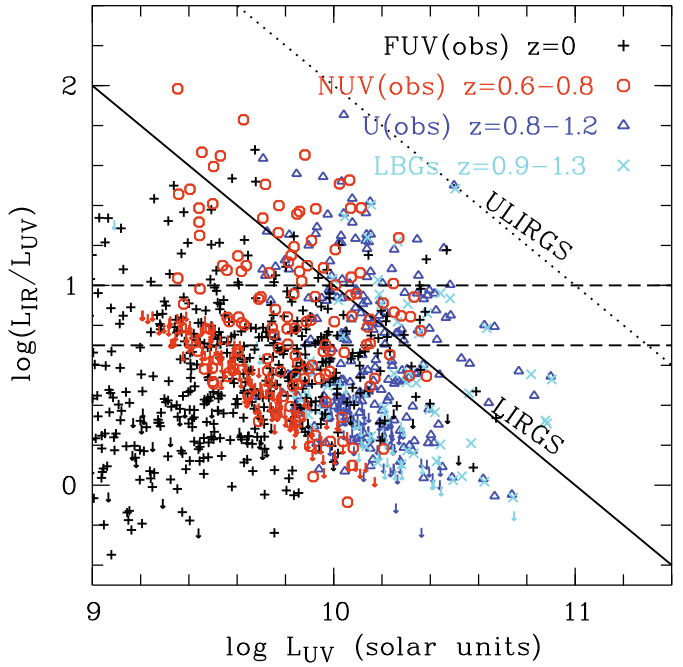

Fig. 4. $\log(L_{IR}/L_{UV})$ versus L_{UV} for the different samples defined in this work. The diagonal solid lines are the limits above which galaxies are LIRGs or ULIRGs.

comparison. However the BM/BX galaxies appear to follow the trend reported for LBGs at $z \simeq 1$.

However the interpretation of this plot is difficult because the quantities reported along the axes are both in terms of L_{IR} and L_{UV}. This is illustrated in Fig. 3, where the galaxies are considered according to their UV luminosity, regardless of their redshift. The lines represent the locus of galaxies with a given L_{UV}. The locus of galaxies in this plot is strongly constrained by their UV luminosity: as L_{IR}/L_{UV} varies, galaxies of a given L_{UV} move along lines such as those overplotted on the diagram. Therefore, the shift seen in Fig. 2 is caused by the presence of more luminous galaxies in UV as z increases as expected from the evolution of the UV luminosity function (Arnouts et al. 2005; Takeuchi et al. 2005b). The variation in dust attenuation measured by L_{IR}/L_{UV}, can only be quantified for data points along these lines of constant L_{UV}.

3.2. L_{IR}/L_{UV} versus L_{UV}

From the above analysis, it is clear that we must avoid combining IR and UV luminosities along both axes, since the resulting plot becomes too tightly constrained. We can analyze the variation of L_{IR}/L_{UV} as a function of L_{UV} alone. In the corresponding plot, we are not affected by volume effects since all the samples are selected in UV. A similar work was performed by Xu et al. (2007) based on shallower data and a stacking analysis. No evolution of L_{IR}/L_{UV} for a given L_{UV} was found from z = 0 to z = 0.6. The variation in L_{IR}/L_{UV} as a function of L_{UV} is reported in Fig. 4. The loci of LIRGs ($L_{IR} > 10^{11}\ L_\odot$) and ULIRGs ($L_{IR} > 10^{12}\ L_\odot$) are also indicated. This time the general shape of this diagram is strongly constrained by the upper limits to 24 μm which prevent any discussion about the low values of L_{IR}/L_{UV}. The upper envelope to the distribution shows a trend: as L_{UV} increases the maximum value of L_{IR}/L_{UV} decreases from ~50 to ~3 (~65 to ~5 for the CE01 calibration). A quantitative interpretation of this varying upper limit is difficult because of the limited statistics: since the total number of galaxies per luminosity bin decreases as the UV luminosity increases, we expect to observe less extreme cases even for a similar parent distribution of L_{IR}/L_{UV}. In all cases, the most UV luminous galaxies exhibit a very moderate dust attenuation of $\log(L_{IR}/L_{UV})$ = 0.5 (which corresponds to A_{UV} = 1.2 mag with the calibration of Buat et al. (2005)), and the galaxies with the largest dust attenuation are the faintest in the UV.

To further interpret Fig. 4 we calculated the fraction of galaxies with $\log(L_{IR}/L_{UV})$ higher than 0.7 and 1 (corresponding to A_{UV} = 1.5 and 2 mag respectively, Buat et al. 2005) as well as the fraction of LIRGs of each redshift, as a function of L_{UV}. The cuts adopted for $\log(L_{IR}/L_{UV})$ (0.7 and 1) are chosen so as not to be affected by the non-detections at 24 μm in the high redshift samples (cf. the upper limits reported in Fig. 4). If the CE01 calibration is used instead of that of TBI05, the cuts in $\log(L_{IR}/L_{UV})$ have to be increased by 0.1 dex (i.e., $\log(L_{IR}/L_{UV})$ = 0.8 and 1.1).

The results are reported in Figs. 5 and 6. At z = 0, all galaxies are detected in IR and the distribution of L_{IR}/L_{UV} is described well by a Gaussian with a mean value of 0.55 dex and a standard deviation of 0.3 dex. If we first consider the fraction of galaxies with $\log(L_{IR}/L_{UV}) > 0.7$, this fraction is not found to be very dependent either on the redshift or the UV luminosity at least up to $\log L_{UV} \leq$ 10.3–10.4 ($L_\odot$) (there is only one discrepant point at z = 0.7, but which also has a very large error bar). For the highest observed UV luminosities ($\log(L_{UV}[L_\odot]) \geq$ 10.3–10.4), which are only present in the samples at $z \simeq 1$, the fraction of galaxies with $\log(L_{IR}/L_{UV}) > 0.7$ decreases both for the U selection and the LBGs. The LBG sample has a slightly lower fraction of galaxies with $\log(L_{IR}/L_{UV}) > 0.7$ than that found in the U-selected sample over the whole range of luminosity.

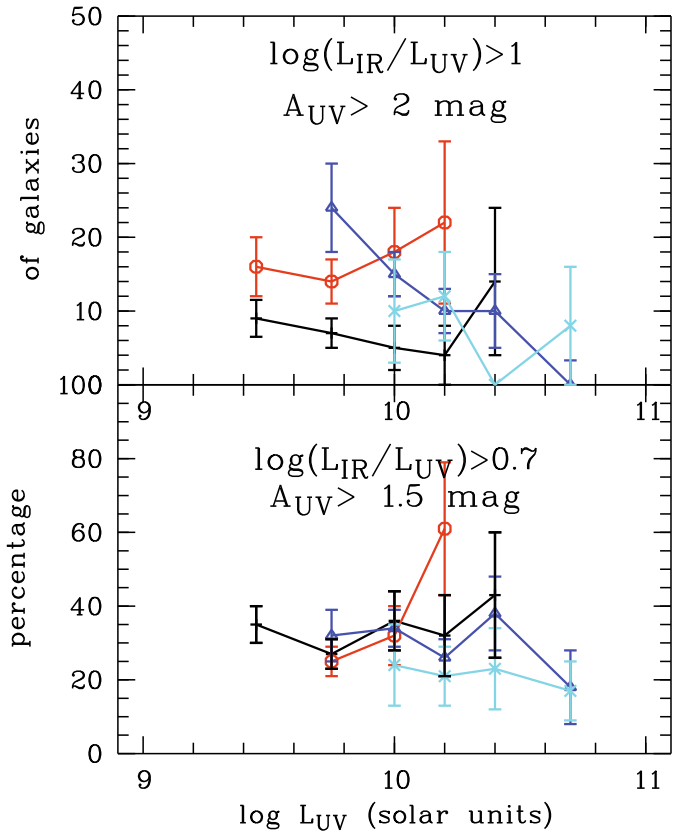

Fig. 5. Fraction of galaxies with $\log(L_{IR}/L_{UV}) > 0.7$, $\log(L_{IR}/L_{UV}) > 1$. The symbols are the same as in Fig. 2. The first bin of luminosity in the *lower panel* is not considered at $z = 0.7$, since the upper limits to $\log(L_{IR}/L_{UV})$ calculated for the galaxies with this luminosity and undetected at 24 μm may be higher than 0.7.

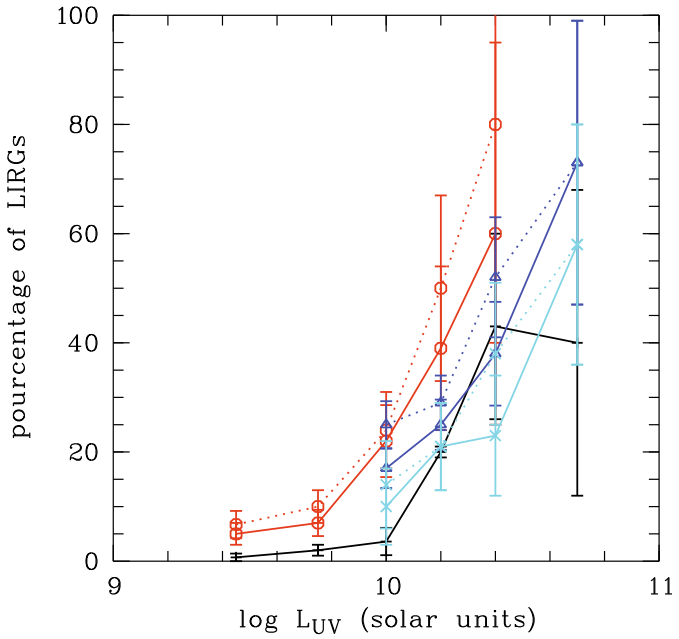

Fig. 6. Fraction of LIRGs, the symbols are the same as in Fig. 2. The solid lines refer to the TBI05 calibration for L_{IR} and the dotted lines to the CE01 calibration.

Galaxies with $\log(L_{IR}/L_{UV}) > 1$ represent those with the highest dust attenuation. This fraction does not exceed ≃20% for all of our samples. Galaxies with such a high extinction seem to be more frequent at $z > 0$ than at $z = 0$: the distribution of L_{IR}/L_{UV} is found to reach higher values at $z > 0$ than at $z = 0$ but we must remain cautious because of the uncertainties in the MIR-total IR calibration. As found above, at $z = 1$ there is almost no UV luminous galaxy with a high dust attenuation and the fraction of galaxies with $\log(L_{IR}/L_{UV}) > 1$ increases toward lower UV luminosities.

The evolution in the fraction of LIRGs is reported in Fig. 6. This fraction increases with UV luminosity: it is expected even without any evolution in the L_{IR}/L_{UV} distribution. For the UV-selected galaxies at $z = 0$, 0.7, and 1, the variations are found similar, there being a slightly higher fraction of LIRGs at a given UV luminosity at $z > 0$, which is the same effect noted for galaxies with $\log(L_{IR}/L_{UV}) > 1$. The fraction of LIRGs in the LBG sample is systematically lower than that found for the UV-selected galaxies at $z = 1$, again leading to the conclusion of lower dust attenuation for these galaxies.

Reddy et al. (2008) estimated the colour excess distribution of BX galaxies at $z \simeq 2$ and LBGs at $z \simeq 3$. They found that $\langle E(B-V)\rangle = 0.15 \pm 0.07$. Adopting the dust attenuation law of Calzetti et al. (2000), we can infer that $\langle A_{UV}\rangle = 1.5$ mag. As a consequence 50% of BX galaxies and LBGs have $A_{UV} > 1.5$ mag, and, if we assume that the distribution of $E(B-V)$ is Gaussian, 30% have $A_{UV} > 2$ mag. Reddy et al. (2008) obtained similar results by analyzing the L_{IR}/L_{UV} distribution. They also found that the average dust attenuation did not vary with UV rest-frame luminosity.

Therefore dust attenuation in UV-selected galaxies at $z > 1$ seems to be slightly higher than that found at $z \simeq 1$, the difference being particularly significant for UV luminous galaxies for which there is a hint of a lower dust attenuation at $z \simeq 1$. Nevertheless, we must remain cautious in our conclusions given the uncertainties in the estimates of dust attenuation and the different methods adopted, i.e., IR to UV flux ratio to $z = 1$ based on 12 and 15 μm luminosities, UV colours and 8 μm luminosities at higher z. These methods are known to provide different results at least up to $z = 1$ (Burgarella et al. 2007; Elbaz et al. 2007) and the calibration of the 8 μm luminosity in terms of total IR luminosity is highly uncertain (Caputi et al. 2007; Burgarella et al. 2009).

3.3. L_{IR}/L_{UV} versus L_K

We have seen that it is difficult to interpret the variation in L_{IR}/L_{UV} as a function of a quantity that also depends on these two luminosities. We can also use a quantity that is independent of them to avoid this problem. We now consider the rest-frame K luminosity of the galaxies, which is a tracer of the stellar mass of galaxies. It is calculated with the IRAC band at 3.6 and 4.5 μm, which corresponds to rest-frame K at $z = 0.7$ and 1, and with 2MASS data at $z = 0$ (Buat et al. 2007a). In Fig. 7 we report the variation in L_{IR}/L_{UV} as a function of L_K for the different samples, also divided in luminosity bins. A net increase in L_{IR}/L_{UV} with L_K is found without any clear evolution with z being evident for the galaxies selected on the basis of their UV rest-frame light, only LBGs appearing to have a lower dust attenuation for a given L_K. When the samples are split according to the UV luminosity of the galaxies, it appears on average that the more UV luminous objects exhibit a lower L_{IR}/L_{UV} for a given K luminosity than UV fainter sources. This agrees with the results in Sect. 3.2. A linear regression fitted to both L_{UV} and L_K infers

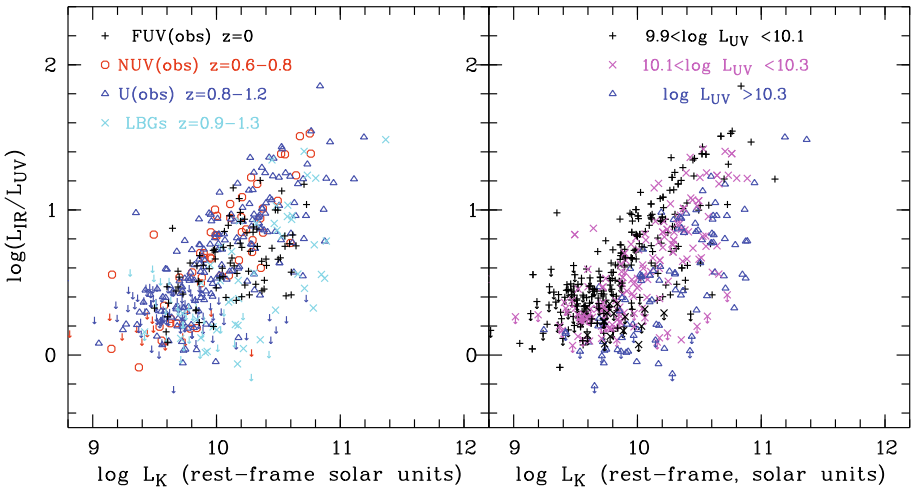

Fig. 7. L_{IR}/L_{UV} versus the K rest-frame luminosity L_K expressed in solar units. *Left panel*: the different samples are plotted with the same symbols as in Fig. 2. *Right panel*: the samples are divided according to the UV luminosity as in Fig. 3.

that

$$\log(L_{IR}/L_{UV}) = 0.78(0.04)\ \log\ L_K - 0.79(0.06)\log L_{UV} + 0.86(0.21). \quad (5)$$

Excluding LBGs from the analysis (since they are less dust-extinguished than UV-selected galaxies) leads to a slightly different regression of

$$\log(L_{IR}/L_{UV}) = 0.78(0.04)\ \log\ L_K - 0.65(0.07)\log L_{UV} - 0.58(0.21). \quad (6)$$

Using the calibration of Chary & Elbaz (2001) we would infer instead

$$\log(L_{IR}/L_{UV}) = 0.81(0.04)\ \log\ L_K - 0.54(0.06)\log L_{UV} - 1.92(0.26) \quad (7)$$

for the whole sample and

$$\log(L_{IR}/L_{UV}) = 0.81(0.04)\ \log\ L_K - 0.54(0.08)\log L_{UV} - 1.91(0.25) \quad (8)$$

when LBGs are excluded.

Martin et al. (2007) and Iglesias-Paramo et al. (2007) also studied the variation in L_{IR}/L_{UV} as a function of the stellar mass from $z = 0$ to 1 for UV-selected galaxies, and our results are globally consistent with theirs: all relations between L_{IR}/L_{UV} and L_K or M_{star} exhibit the same steepness, and the shift with redshift reported in these studies is of similar amplitude to the one we find as a function of L_{UV}. The main differences between these previous analyses and ours is that we select galaxies to the same limit in UV luminosity whereas the other studies were based on magnitude-limited samples with a different limit in luminosity as z varies. Our approach allows us to emphasise differences in the behaviour as a function of galaxy luminosity and this effect seems to be at the origin of the redshift evolution reported earlier.

4. Star-formation activity

Dust attenuation was found to be related to the observed UV and K luminosity of our UV-selected galaxies, LBGs exhibiting a more extreme behaviour. Is the strength of the star-formation activity also linked to the UV luminosity? Do LBGs exhibit a different star-formation activity than UV-selected galaxies? The star-formation activity can be quantified in terms of the specific star formation rate (SSFR), defined to be the ratio of the current star-formation rate to the stellar mass of the galaxies. We can estimate this quantity with our data sets. We calculate the total SFR by adding the SFR from the IR and the UV (observed) luminosities (Iglesias-Paramo et al. 2006; Buat et al. 2008). We adopt a Salpeter IMF and the formulae of Iglesias-Paramo et al. (2006), i.e.,

$$\log\ SFR_{IR}(M_\odot\,\mathrm{yr}^{-1}) = \log L_{IR}(L_\odot) - 9.75 \quad (9)$$

$$\log\ SFR_{UV}(M_\odot\,\mathrm{yr}^{-1}) = \log L_{UV}(L_\odot) - 9.51. \quad (10)$$

The total SFR is expressed as $SFR_{IR} + SFR_{UV}$ except at $z = 0$, where the contribution of the dust emission is not related to the star formation, which is estimated to be 30% (Iglesias-Paramo et al. 2006). The stellar masses of the galaxies are calculated with the IRAC band at 3.6 and 4.5 μm, which corresponds to rest-frame K-band at $z = 0.7$ and, adopting the calibration of Arnouts et al. (2007). At $z = 0$, the calibration of Bell et al. (2003) is used as discussed in Iglesias-Paramo et al. (2006) and Buat et al. (2008). We adopt a Salpeter IMF and check that the extrapolation of the calibration of Arnouts et al. (2007) is consistent with that we adopt at $z = 0$, within to 30% (0.1 dex).

In Fig. 8, we report the variation in SSFR as a function of the stellar mass for each sample truncated at $\log L_{UV} > 9.9\ (L_\odot)$. This limit when combined with the detection limit adopted for the fluxes at 24 μm (25 μJy) infers a limit in SFR at $z = 0$ and 1, also indicated in Fig. 8. The SSFR at a given stellar mass increases with z, as reported in both observational and theoretical studies and predicted in scenarios of galaxy evolution. The SSFR also exhibits a flat distribution: it is expected when only star-forming galaxies are selected (Elbaz et al. 2007; Buat et al. 2008). The consistency between models and the mean trends found in UV and IR selected samples was shown to be good up to $z = 0.7$ (Buat et al. 2008) but breaks at $z \geq 1$ (Elbaz et al. 2007). The purpose of this paper is not to perform a comparison between models and observations since we are dealing with only a subsample of the overall galaxy population: the objects with $\log L_{UV} > 9.9(L_\odot)$. We want to compare the properties of these galaxies at different z, and with those of LBGs. LBGs and UV-selected galaxies seem to experience similar SSFRs at the same redshift. We now focus on the most massive galaxies with $\log(M_{star}) > 10.8(M_\odot)$ for which the detection limits reported in Fig. 8 do not produce a substantial bias. The galaxies of this subsample with a moderate UV luminosity ($\log L_{UV} < 10.4\ (L_\odot)$) exhibit a wide range of SSFRs, the most quiescent objects being found at $z = 0$. In contrast, all the most UV luminous objects

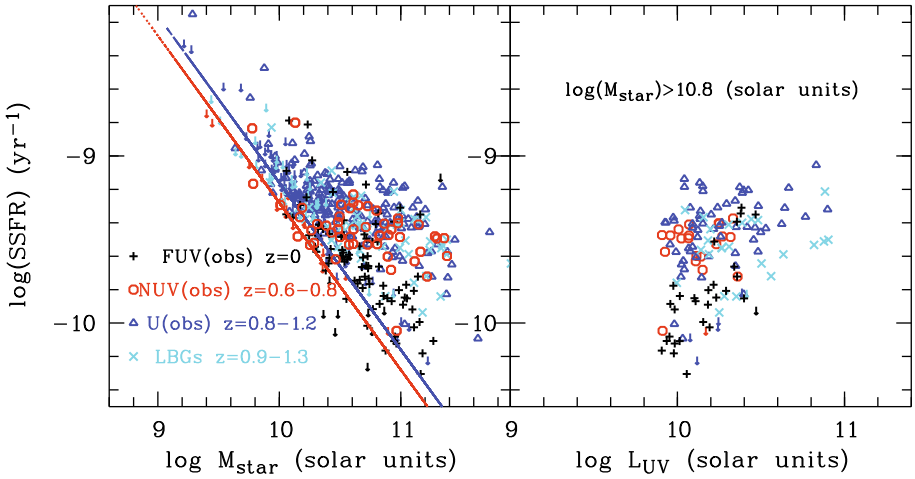

Fig. 8. Variations in the specific star formation rate for each sample considered in this work; all samples are truncated at $\log L_{\rm UV} > 9.9$ in solar units. *Left panel*: as a function of the stellar mass of the galaxies. The diagonal lines are the lower limits to SSFR for $z = 0.7$ (lower line) and 1 (upper line). *Right panel*: as a function of the UV luminosity for galaxies with $\log(M_{\rm star}) > 10.8(M_\odot)$.

($\log L_{\rm UV} > 10.4$ ($L_\odot$)) exhibit quite high SSFRs. These galaxies have SFRs of between 10 and 190 $M_\odot$ yr^{-1} with an average value of 55 $M_\odot$ yr^{-1}: at this rate they might have formed all their mass in a few Gyr.

5. Total UV + IR luminosity functions

Are we missing star-forming galaxies with a UV selection to $z = 1$, and as a consequence are we able to measure all the star formation when applying a reliable dust attenuation to galaxies selected in UV rest frame? To answer these questions, we need to construct the luminosity functions (LFs) of the total luminosity, related to star formation activity, $L_{\rm UV} + L_{\rm IR}$.

5.1. Method

The most important but difficult point of this analysis is how to handle the two variables $L_{\rm UV}$ and $L_{\rm IR}$ at the same time. We proceed with our statistical analysis as follows:

Step 1: since our sample is primarily selected at UV (GALEX *FUV* at $z = 0$ taken as reference ($\lambda = 1530$ Å), GALEX *NUV* at $z = 0.7$ and EIS U-band at $z = 1$), we construct univariate UV LFs.

Step 2: we bin the UV LFs, and estimate the distribution of the total IR luminosity estimated by Eqs. (3) and (4) at each bin.

Step 3: we sum the distribution functions of the total IR luminosity along all the UV luminosity bins.

For step 1, we used improved versions of two representative LF estimators: $1/V_{\rm max}$-estimator (Schmidt 1968) and C^--estimator (Lynden-Bell 1971) in an optimal manner, explained and examined extensively by Takeuchi et al. (2000) and Takeuchi (2000). We estimated the LFs of *NUV*-selected sample at $0.6 < z. < 0.8$, U-band selected sample at $0.8 < z < 1.2$, and LBG samples $0.9 < z < 1.3$. Since we are interested in star-forming galaxies, we omitted known quasar/AGN from our sample, as already explained in Sect. 2.1. These univariate UV LFs are estimated in terms of their primary selection bands for both the *NUV*-selected $z = 0.7$ sample and U-band selected $z = 1.0$ sample: we obtain LFs at ∼1400 Å and ∼1800 Å for $z = 0.7$ and 1 respectively. As discussed in Sect. 2.1, the *NUV* and U selected samples correspond to rest-frame wavelengths that are close enough for K-corrections to be unnecessary. This is not the case for the LBG sample primarily selected in *NUV* which corresponds to ∼1100 Å rest-frame. We return to this issue in Sect. 5.2.

In step 2, we should carefully consider the significant number of upper limits at MIPS 24 μm. For this, we use the Kaplan-Meier estimator, which enables us to use the information content carried by the upper limits, originally developed in the field of lifetime data analysis (Kaplan & Meier 1958). Another desirable property of the Kaplan-Meier estimator is that we can obtain its variance in an analytic form. Formulations, derivations, and some important properties will be discussed and explained elsewhere (Takeuchi et al. 2009, in preparation).

In step 3, statistical errors are summed in quadrature, i.e., the variance from the primary univariate UV LF and that from the IR luminosity distributions. However, we did not include the variance caused by the density inhomogeneity of galaxies (often referred to as cosmic variance), which we discuss in Sect. 5.2.

5.2. UV luminosity functions

We show the UV LFs for the samples at $z = 0.7$ and 1 in Fig. 9. Since both $1/V_{\rm max}$ and C^--estimates agree very well with each other, we only show the latter in this paper. We also estimated the UV LF of LBGs, but it is not obtained by the same method as the other two LFs, since the primary selection was completed in *NUV* (which, for the redshift range of $0.9 < z < 1.3$, corresponds to 1100 Å). Therefore we must use a bivariate method, as described in step 2 above: we first construct a univariate UV LF at 1100 Å, then construct distributions of UV luminosities at each bin from the U-band data (∼1700 Å at the rest-frame), and sum them up within each UV luminosity bin. The obtained UV LF of LBGs is presented in cyan symbols in Fig. 9.

Roughly speaking, we observe that the UV LFs at redshift ranges of $z = 0.7$ and $z = 1.0$ agree with those of Arnouts et al. (2005). This shows that our selection is appropriate to this study. Some discrepancies can be seen between the shapes of our UV LFs and those of Arnouts et al. (2005). may be attributed to the difference in the selection of galaxies, e.g., Arnouts et al. (2005) performed a *NUV* selection and K-corrected the flux, unlike our selection which was for U-band at $z = 1$, without K-correction. The different way in which photometry was performed may also be at the origin of subtle differences: the GALEX deep fields are known to be crowded for *NUV* > 23 mag, Sextractor does not accurately separate these sources leading, to an under-density and a brightening of sources. In the U-band the PSF is smaller, so less or not affected by confusion.

We then focus on the difference between the UV LF derived from U-band data and the LBG LF. As mentioned above,

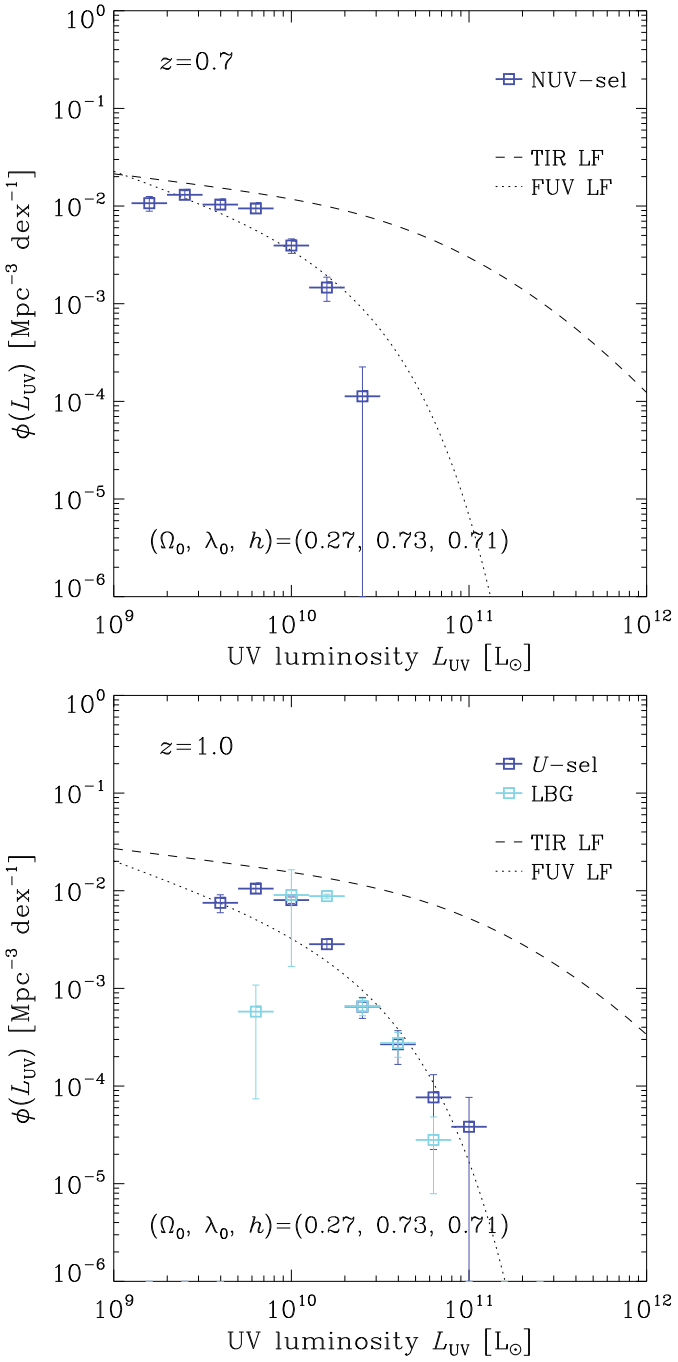

Fig. 9. The UV (1600 Å LFs of the sample at $z = 0.7$ and $z \simeq 1.0$ (U-selected sample and LBGs).

the former was constructed with the U-band selection with the univariate method, while the latter was constructed by the bivariate method, i.e., we first select galaxies at *NUV*, with a *FUV-NUV* colour criterion, and then we estimate the U-band luminosity distribution. Therefore, LBG selection criteria at $z = 1.1$ do not differ strongly from the U-selection at similar redshift ($z = 1$), since both are based on a UV rest-frame selection. Nevertheless, in the LBG selection we miss UV-faint galaxies at $L_{\rm UV} < 10^{10}\ L_\odot$ compared to the U-selection, probably because of the combined effects of a selection at a shorter rest-frame wavelength for the LBGs and a *FUV-NUV* criterion that selects only blue objects, as explained in Sect. 2.2. This suggests that the LBG selection criterion is likely to select UV-luminous galaxies. We return to this point when we discuss the difference between the total UV + IR luminosity functions.

5.3. The total UV + IR luminosity functions

Here, we present the total UV + IR LFs from our UV-selected samples. We again emphasize that we considered the upper limits to the sample at MIPS 24 μm using the Kaplan-Meier method, i.e., we have made a maximal use of the observed information from IR. We show the total LFs in Fig. 10. The top panel shows the $L_{\rm UV} + L_{\rm IR}$ LF at $z = 0.7$, while bottom panel is the one at $z = 1.0$. In Fig. 10, we also show the univariate UV LFs constructed from purely UV-selected samples by Arnouts et al. (2005) (dotted lines), as well as univariate IR LFs compiled from purely IR-selected samples at 24 μm by Le Floc'h et al. (2005) (dashed lines). The symbols are the LFs derived from our sample. Errors are calculated analytically by the asymptotic variance formula of the Kaplan-Meier estimator, convolved with the statistical error in the univariate LFs at UV. The indicated errors are 1σ (68% CL). Because of the known limitation of the Kaplan-Meier estimator, the lowest luminosity bins are underestimated (as indicated by arrows on the symbols).

Clearly, the total LFs are much higher in value than the univariate UV LFs. This means that most of the luminosity of a galaxy at these redshifts is emitted in the IR. Since the luminosity related to their star formation activity tends to be emitted in the IR wavelengths (e.g., Takeuchi et al. 2005b), the resulting total LFs is consistent with this findingt.

At $z = 0.7$, the total LF is even higher than the IR LF of Le Floc'h et al. (2005), but within the uncertainty level related to cosmic variance (~60% for GOODS: Somerville et al. 2004). Apart from this, it is rather consistent with the IR LF. This is an expected higher-z counterpart of the result discussed by Buat et al. (2007a) at $z = 0.0$.

In contrast, the total LF is significantly lower than the IR LF at $z = 1.0$ for galaxies more luminous than $\simeq 2 \times 10^{11}\ L_\odot$. It is worth mentioning that the primary UV LF has an excess in its normalisation compared to the global univariate UV LF at the same redshift. This deficiency of galaxies turns out to be quite significant. Although the most luminous bin is significantly affected by the symbol with a very large error, we see a trend in which the more luminous galaxies are, the larger the discrepancy becomes. This is a clear piece of evidence that our UV-selection misses intrinsically luminous galaxies which are actively star-forming. These galaxies should be studied by means of an IR selection. Buat et al. (2007a) considered both IR and UV selections in the nearby universe and found that the more luminous galaxies (in terms of total $L_{\rm UV} + L_{\rm IR}$ luminosity) are present in the IR selection and experience a very strong dust attenuation. Galaxies more luminous than $\simeq 2 \times 10^{11}\ L_\odot$ exhibit a mean $\log(L_{\rm IR}/L_{\rm UV}) \gtrsim 2$. The relation found between $L_{\rm UV} + L_{\rm IR}$ and $L_{\rm IR}/L_{\rm UV}$ at $z = 0$ has been found to be globally valid at higher z for IR selections (Choi et al. 2006; Xu et al. 2007; Zheng et al. 2006). An $L_{\rm IR}/L_{\rm UV}$ ratio higher than 100 for galaxies more luminous than $\simeq 2 \times 10^{11}\ L_\odot$ implies that these galaxies are not detected at $z = 1$ in our U selection (which is limited to $\log(L_{\rm UV}[L_\odot]) > 9.9$.)

At $z = 0.7$, our UV selection goes deeper ($\log(L_{\rm UV}[L_\odot]) > 9.3$), therefore galaxies with a higher dust attenuation can be detected in UV. We note that galaxies with the highest $L_{\rm IR}/L_{\rm UV}$ are found at $z = 0.7$ (Fig. 4) for the UV faintest galaxies and that the fraction of galaxies with $\log(L_{\rm IR}/L_{\rm UV}) > 1$ is globally higher at $z = 0.7$ than at any other redshift (Fig. 5). However, a drastic evolution from $z = 0.7$ to $z = 1.0$ would be puzzling. Since the

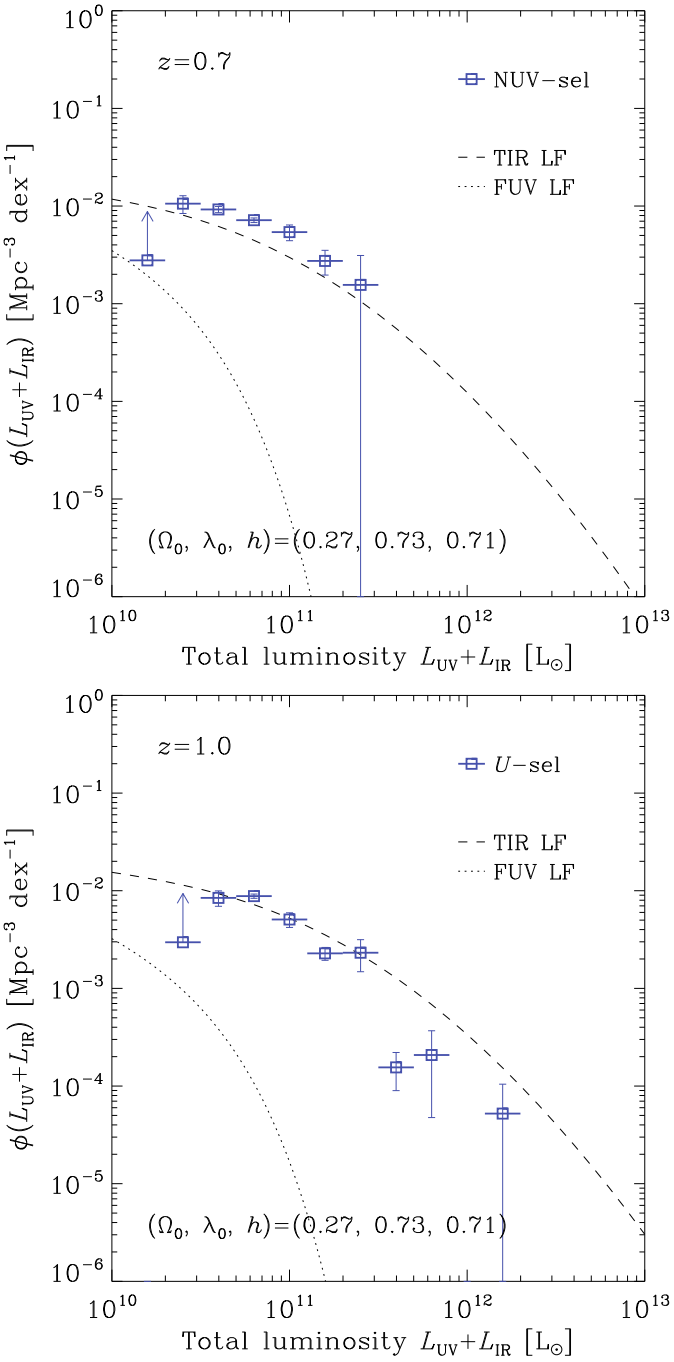

Fig. 10. The total $L_{\rm UV}$ + $L_{\rm IR}$ luminosity functions at z = 0.7 and 1. We also show univariate UV LFs constructed from purely UV-selected samples by Arnouts et al. (2005) (dotted lines), as well as univariate IR LFs made from purely IR-selected samples at 24 μm by Le Floc'h et al. (2005) (dashed lines). The symbols are the LFs derived from our sample. The indicated errors are 1σ (68% CL).

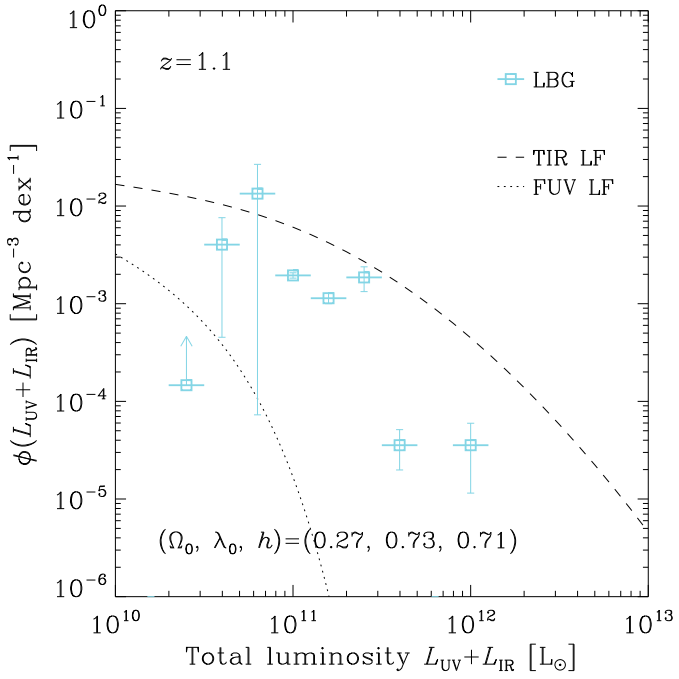

Fig. 11. The total $L_{\rm UV}$ + $L_{\rm IR}$ LF of the LBG sample. The open squares represent the total LF of LBGs. Other symbols are the same as in Fig. 10.

cosmic time differs by less than a few Gyr, this evolution would be very rapid.

As a conclusion, up to z = 1 UV rest-frame observations must be much deeper (by more than 5 mag) than the expected limit in bolometric luminosities, if one is to be able to detect most of the star-forming galaxies.

Figure 11 shows the total UV + IR LF of the LBG sample. The deficiency of total LF is more prominently seen in the LBG LF. In this case, the deficiency extends toward lower luminosities $\simeq 4 \times 10^{10}$ $L_\odot$. Considering the LBG sample selection which makes use of *NUV* and *FUV* fluxes observed at 2310 and 1530 Å by GALEX, this trend may be understood consistently: the LBG sample consists of galaxies with less extinction on average, leading to lower IR luminosities with respect to the same $L_{\rm UV}$ as shown in Sect. 3. The deficiency with respect to the U-selection affects the faintest bins of the LBG LF (Fig. 9 and discussion in Sect. 5.2). Since the dispersion of the $L_{\rm IR}/L_{\rm UV}$ distribution is very large as we have seen before, the contribution of these bins to the number density of galaxies is significant, and the deficiency of galaxies affects all the range of the total UV + IR LF.

5.4. Discussion

As discussed by many authors (e.g., Chary & Elbaz 2001; Takeuchi et al. 2005a; Caputi et al. 2007; Rieke et al. 2008), the monochromatic MIR luminosity-to-total IR luminosity conversion plays an important role, especially because of the limited number of deep multi-band observations at FIR. Since the intrinsic scatter in the linear regression is not very small, these "calibration formulae" inevitably have significant uncertainty. It makes then sense to examine how different formulae affect our results, especially the deficiency of intrinsically luminous galaxies in the UV-selection.

To test this, we estimated the total UV + IR LFs in exactly the same manner but with CE01 conversion. The resulting LFs are shown in Fig. 12. In Fig. 12, open squares represent the LFs with the formula of Takeuchi et al. (2005a), while open triangles are those with CE01 conversion. All the other symbols are the same as in Fig. 10.

At z = 0.7, since the difference of these formulae is quite small (cf. upper panel in Fig. 1), the results are almost the same. At z = 1.0, the difference is visible between the two estimates. As we have seen in Fig. 1, CE01 formula infers a higher IR luminosity. Hence, it produces higher total luminosity in $L_{\rm UV}+L_{\rm IR}$ than for the same $L_{\rm UV}$. As a result, the discrepancy between the

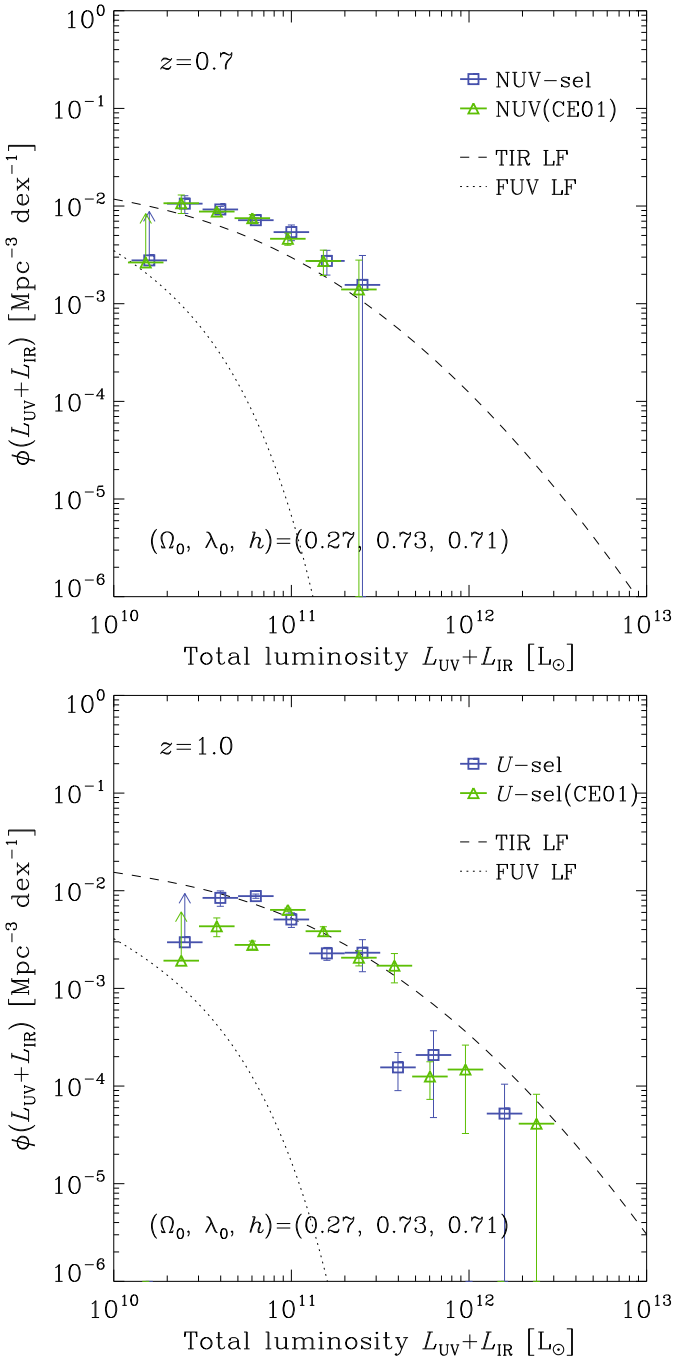

Fig. 12. Comparison between the total LFs with the L_{IR} estimator of Takeuchi et al. (2005a) and those with Chary & Elbaz (2001).

total LF and the IR LF becomes smaller, but still statistically significant.

At $z \simeq 2$ and $\simeq 3$, Reddy et al. (2008) were able to reproduce all the IR LF up to $L_{IR} = 10^{12}\ L_{\odot}$ from only UV-optical data with an excess of faint sources compared to results from IR surveys alone. They constructed the UV rest-frame LF with Monte Carlo simulations to recover all the star-forming galaxies; to recover the IR LF, they then assumed either a constant dust attenuation distribution irrespective of UV luminosity or a decrease in the average dust attenuation for UV faint galaxies. in contrast, at $z \simeq 1$ dust attenuation is found not to be very dependent on UV luminosity with only a slight decrease for UV luminous galaxies. We cannot reconstruct the bright end of the IR LF from a UV-selected sample. The IR luminous galaxies, observed in IR surveys, exhibit a very high dust attenuation which makes them undetected in UV (rest-frame). Since we use observed IR and UV flux densities (including upper limits), our method can be considered to be robust, although it is dependent on the validity of the MIR to total IR luminosity conversion. The method of Reddy et al. also suffers from the uncertainty in the MIR to total IR luminosity conversion, which is particularly large at 8 μm rest-frame, and on the accuracy of dust attenuation factors estimated from the UV-optical alone (see discussion in Sect. 3.2). Nevertheless if we trust both results, together they imply that there is a lower fraction of galaxies intrinsically UV+IR luminous and with a large dust attenuation is found at $z \simeq 2$–3 than at $z \simeq 1$. We will reinvestigate this issue by using IR-selected samples up to $z = 1$ in a fully bivariate manner (Takeuchi et al. 2009, in preparation). The future observations of Herschel should give us the high redshift IR selected samples necessary to solve this question.

6. Conclusions

We have analysed the IR emission of galaxies selected in UV rest-frame from $z = 0$ to $z = 1$. The samples were carefully selected to ensure that they were very homogeneously selected in terms of wavelength and luminosities. We also considered a sample of Lyman break galaxies at $z \simeq 1$.

1. The L_{IR}/L_{UV} ratio was used as a proxy for dust attenuation. For the bulk of our galaxy samples, this dust attenuation is found not to vary significantly with z, and fewer than 20% of the sample galaxies have a $L_{IR}/L_{UV} > 10$. Some evolution is seen in the extreme regimes of high and low L_{IR}/L_{UV} ratio. The most luminous UV objects ($L_{UV} \simeq 2 \times 10^{10}\ L_{\odot}$) are only present at $z = 1$ and exhibit very low dust attenuation. When $L_{UV} \lesssim 2 \times 10^{10}\ L_{\odot}$, the fraction of galaxies with a high L_{IR}/L_{UV} is larger at $z > 0$ than in the nearby universe, and the galaxies with the highest dust attenuation are the faintest ones in our samples ($L_{UV} \simeq 3 \times 10^{9}\ L_{\odot}$). However, these results all depend on the MIR-total IR calibration, which is uncertain. Dust attenuation increases with the K luminosity in a similar way at all redshifts. A residual trend is found with UV luminosity: as L_{UV} increases, galaxies of a given L_K have a lower L_{IR}/L_{UV}. A relation between L_{IR}/L_{UV}, L_{UV} and L_K is given. At $z = 1$, LBGs seem to be less affected by dust attenuation than UV-selected galaxies of similar UV luminosity and at same z. Since the UV luminosity of galaxies globally increases with z, these trends found with the UV luminosity must be accounted for to interpret the evolution with redshift of L_{IR}/L_{UV} reported in previous studies.
2. Massive and UV luminous galaxies ($\log(M_{star}) > 10.8(M_{\odot})$ and $\log L_{UV} > 10.4\ (L_{\odot})$) are found to be very active in star formation (high SSFR), whereas fainter galaxies of similar mass exhibit a wider range of SSFR. LBGs and UV-selected galaxies have similar SSFR.
3. We have constructed LFs for the total luminosity related to star-formation activity, $L_{UV} + L_{IR}$ from our UV-selected galaxy samples. We have used the Kaplan-Meier estimator to use information carried by IR detections and upper limits in a coherent manner. The resulting total UV+ IR LFs are much higher than the univariate UV LFs from purely UV-selected samples. This means that most of the luminosity produced by star formation activity is emitted in the IR wavelength range. Although, at $z = 0.7$, the total LF we obtain is consistent (even higher because of a density excess) with the

univariate IR LF, we have found a clear deficiency of galaxies in the total LF at $z = 1.0$, for galaxies more luminous than $\simeq 2 \times 10^{11}\ L_{\odot}$ This result is not significantly affected by a different total IR luminosity calibration formula. Thus, we conclude that the IR LF cannot be reconstructed solely from our UV-selected galaxies at $z = 1$ and that deeper data are needed to detect galaxies with a high $L_{\rm IR}/L_{\rm UV}$. Practically, to detect most of the star-forming galaxies to a given bolometric magnitude faintness level, UV rest-frame observations must be deeper than this bolometric limit by at least 5 mag (corresponding to ($L_{\rm IR}/L_{\rm UV} \simeq 100$). The deficiency in the total LF is found to be much higher for the LBG selection affecting the entire range of luminosity explored in this work for these objects (i.e., $\gtrsim 4 \times 10^{10}\ L_{\odot}$).

Acknowledgements. T.T.T. has been supported by Program for Improvement of Research Environment for Young Researchers from Special Coordination Funds for Promoting Science and Technology, and the Grant-in-Aid for the Scientific Research Fund (20740105) commissioned by the Ministry of Education, Culture, Sports, Science and Technology (MEXT) of Japan. We thank Akio K. Inoue and Hiroyuki Hirashita for fruitful discussions. TTT and KLM are partially supported from the Grand-in-Aid for the Global COE Program "Quest for Fundamental Principles in the Universe: from Particles to the Solar System and the Cosmos" from the MEXT.

References

Arnouts, S., Vandame, B., Benoist, C., et al. 2001, A&A, 379, 740
Arnouts, S., Schiminovich, D., Ilbert, O., et al. 2005, ApJ, 619, L43
Arnouts, S., Walcher, C. J., Le Fèvre O., et al. 2007, A&A, 476, 137
Basu-Zych, A. R., Schiminovich, D., Johnson, B., et al. 2007, ApJS, 173, 457
Bauer, F. E., Alexandern, D. M., Brandt, W. N., et al. 2004, AJ, 128, 2048
Bell, E. F., MacIntosh, D. H., Katz, N., & Weinberg, N. D. 2003, ApJS, 149, 289
Buat, V., Deharveng, J. M., Burgarella, D., & Kunth, D. 2002, A&A, 393, 33
Buat, V., Iglesias-Páramo, J, Seibert, M., et al. 2005, ApJ, 619, L51
Buat, V., Takeuchi, T. T., Iglesias-Páramo, J, et al. 2007a, ApJS, 173, 404
Buat, V., Marcillac, D., Burgarella, D., et al. 2007b, A&A, 469, 19
Buat, V., Boissier, S., Burgarella, D., et al. 2008, A&A, 483, 107
Burgarella, D., Pérez-González, P., & Tyler, K. D. 2006, A&A, 450, 69
Burgarella, D., Le Floc'h, E., & Takeuchi, T. T. 2007, MNRAS, 380, 986
Burgarella, D., Buat, V., & Takeuchi, T. T. 2009, PASJ, 61, 177
Calzetti, D., Armus, L., Bohlin, R. C., et al. 2000, ApJ, 533, 682
Caputi, K, Lagache, G., Yan, L., et al. 2007, ApJ, 660, 97
Chary, R., & Elbaz, D. 2001, ApJ, 556, 562
Choi, P. I., Yan, L., Im, M., et al. 2006, ApJ, 637, 227
Dale, D. A., & Helou, G. 2002, ApJ, 576, 159
Dale, D. A., Helou, G., Contursi, A., et al. 2001, ApJ, 549, 215
Dale, D. A. , Bendo, G. J., Engelbracht, C. W., et al. 2005, ApJ, 633, 857
Elbaz, D., Daddi, E., Le Borgne, D., et al. 2007, A&A, 468, 33
Heckman, T. M., Hoopes, C. G., Seibert, M., et al. 2005, ApJ, 619, L35
Hoopes, C. G., Heckman, T. M., Salim, S., et al. 2007, ApJS, 173, 441
Hopkins, A. M., Connolly, A. J., Haarsma, D. B., & Cram, L. E. 2001, AJ, 122, 288
Iglesias-Páramo, J., Buat, V., Takeuchi, T. T., et al. 2006, ApJS, 164, 38
Iglesias-Páramo, J., Buat, V., Hernández-Fernández, J., et al. 2007, ApJ, 670, 279
Kaplan, E. L., & Meier, P. 1958, J. Am. Stat. Assoc. 53, 457
Le Floc'h, E., Papocich, C., & Dole, H. 2005, ApJ, 632, 169
Leitherer, C., Li, I.-H, Calzetti, D., & Heckman, T. M. 2002, ApJS, 140, 303
Lynden-Bell, D. 1971, MNRAS, 155, 95
Malkan, M., Webb, W., & Konopacky, Q. 2003, ApJ, 598, 878
Marcillac, D., Elbaz, D., Chary, R. R., et al. 2006, A&A, 451, 57
Martin, D. C., Seibert, M., Buat, V., et al. 2005, ApJ, 619, L59
Martin, D. C. Small, T., Schiminovich, D., et al. 2007, ApJS, 173, 415
Morrissey, P., Schiminovich, D., & Barlow, T. A. 2005, ApJ, 619, L7
Moustakas, J., Kennicutt, R. C., & Tremonti, C. A. 2006, ApJ, 642, 775
Reddy, N. A, Steidel, C. C., & Erb, D. K. 2006, ApJ, 653, 1004
Reddy, N. A., Steidel, C. C., Pettini, M., et al. 2008, ApJS, 175, 48
Rieke, G. H., Alonso-Herrero, A., Weiner, B. J., et al. 2009, ApJ, 692, 556
Saunders, W., Sutherland, W. J., Maddox, S. J., et al. 2000, MNRAS, 317, 55
Schmidt, M. 1968, ApJ, 151, 393
Somerville, R. S., Lee, K., Ferguson, H. C., et al. 2004, ApJ, 600, L171
Stern, D., Eisenhardt, P., Gorjian, V., et al. 2005, ApJ, 631, 163
Takeuchi, T. T. 2000, Ap&SS, 271, 213
Takeuchi, T. T., Yoshikawa, K., & Ishii, T. T. 2000, ApJS, 129, 1
Takeuchi, T. T., Yoshikawa, K., & Ishii, T. T. 2003, ApJ, 587, L89
Takeuchi, T. T., Buat, V., Iglesias-Páramo, J., Boselli, A., & Burgarella, D. 2005a, A&A, 432, 423
Takeuchi, T. T., Buat, V., & Burgarella, D. 2005b, A&A, 440, L17
Tresse, L., Ilbert, O., Zucca, E., et al. 2007, A&A, 472, 404
Wolf, C., Meisenheimer, K., Kleinheinrich, M., et al. 2004, A&A, 421, 913
Xu, C. K., Shupe, D., Buat, V., et al. 2007, ApJS, 173, 432
Zheng, X. Z., Bell, E. F., Rix, H.-W., et al. 2006, ApJ, 640, 784